Fuel Communications 11 (2022) 100068

Contents lists available at ScienceDirect

Fuel Communications

journal homepage: www.sciencedirect.com/journal/fuel-communications

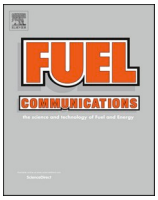

Ignition and combustion characteristics of diesel piloted ammonia injections

Valentin Scharl *, Thomas Sattelmayer

Chair of Thermodynamics, Technical University of Munich, Boltzmannstrae 15, Garching 85748, Germany

ARTICLE INFO

Keywords:
Ammonia
Experimental
Direct-Injection
Combustion
2010 MSC:
00-01
99-00

ABSTRACT

Ammonia is considered a potential carbon-free alternative to fossil fuels. However, its unfavorable combustion characteristics and propensity to form fuel NO_x pose a challenge for its use as fuel for internal combustion engines. The high-pressure dual fuel (HPDF) direct-injection of ammonia could offer the potential to reduce ammonia slip and decrease NO_x formation. The feasibility of this combustion process has not yet been shown experimentally in literature. This work examines the ignition and combustion characteristics of diesel piloted liquid ammonia sprays under engine-relevant conditions in a rapid-compression-expansion-machine (RCEM). By examining heat release rates (HRRs) under a variety of spatial and temporal spray interaction configurations, charge conditions as well as different diesel pilot amounts and injection durations, the fundamental prerequisites for successful combustion of liquid ammonia sprays are revealed. Strong interaction of the two fuels is found necessary to properly ignite ammonia. Misfiring due to deterioration of the pilot mixture formation can be avoided by injecting diesel first. A strong correlation between main ignition delay and burnout rate suggests a significant influence of wall quenching effects. An investigation of less reactive charge conditions suggests poor suitability of the combustion process for low-load engine operation. While reliable ammonia ignition was achieved for diesel pilot amounts as small as 3.2% of the total injected LHV, ignition is increasingly delayed for smaller pilot amounts. For an operating point, which showed favorable ignition behavior and high conversion rates, pilot fuel amount and injection duration are found to have a major influence on the combustion process.

1. Introduction

Climate change and resulting policies increase the demand for power generation and transportation concepts with reduced greenhouse gas emissions. Synthetic fuels offer high energy densities and low-cost storage, which makes them promising for long-range transportation applications and long-term power storage. Due to its carbon free structure, a higher volumetric energy density than hydrogen as well as the existing infrastructure, the interest in ammonia has been growing rapidly in the past years. In particular the shipping industry is working on the adoption of ammonia as a fuel [1]. One major challenge for establishing ammonia as fuel is its poor combustion behavior. The characteristics that present the largest problems are the high energy of evaporation, low flame speed, high auto-ignition temperature and narrow flammability limits [2]. In addition, the combustion of ammonia in internal combustion engines shows a high propensity to form hazardous NO, NO_2 and the potent greenhouse gas N_2O [3,4].

As the combustion of pure ammonia in air has been shown to suffer from incomplete combustion [5,6], several combustion strategies have been investigated to overcome the unfavorable combustion characteristics. Comprehensive reviews can be found in Lesmana et al. [7], Dimitriou and Javaid [8]. A short overview of previous approaches to ammonia combustion in reciprocating engines is given in the following.

Both spark ignition (SI) as well as compression ignition (CI) engines have been adapted to run on ammonia. Several studies use hydrogen to increase the reactivity of the fuel mixture in SI engines. Hydrogen can be obtained by the catalytic dissociation of ammonia into hydrogen and nitrogen before submission into the engine [9,10]. Alternatively, hydrogen/ammonia mixtures are directly used as SI engine fuel [4,11]. Instead of hydrogen, gasoline has been used as a combustion promoter [12]. Even the combustion of pure ammonia has been demonstrated by adopting CI engines with high compression ratios to SI engines by adding a spark plug [2,13]. Several researchers have investigated dual fuel operation with homogenous ammonia air mixtures and a pilot fuel such as diesel, biodiesel or dimethyl-ether (DME) for CI engines [14–18]. Studies from Iowa State University have been considering

* Corresponding author.
E-mail addresses: valentin.scharl@tum.de (V. Scharl), sattelmayer@td.mw.tum.de (T. Sattelmayer).

https://doi.org/10.1016/j.jfueco.2022.100068
Received 19 January 2022; Received in revised form 20 April 2022; Accepted 6 May 2022
Available online 14 May 2022

liquid direct-injection of ammonia mixtures with Diesel or DME [19,20]. Early injection timings and an injector based on spark ignition direct-injection technology were used for the investigation. The homogenous charge compression ignition of ammonia/hydrogen mixtures has also been shown to be feasible [21]. Thereby, the high unburned ammonia emissions were shown to be caused by the large quenching distance near the cylinder wall. In summary, current approaches to ammonia combustion are based on homogenous ammonia/air mixtures and suffer from high unburned ammonia and NO_x emissions.

Unburned fuel slip due to near-wall quenching can be reduced by injecting the main fuel close to top dead center (TDC), while using a secondary, higher cetane number pilot fuel (e.g., diesel) as ignition source. This high-pressure dual fuel (HPDF) combustion has first been demonstrated with methane as the main fuel, which was ignited by a slightly advanced diesel pilot injection [22]. Similar to conventional diesel combustion, the main fuel burns in a predominantly diffusive manner. However, by delaying the diesel injection timing, a partially premixed combustion behavior can be obtained. In addition, the diffusive burnout of ammonia flames might, in contrast to conventional hydrocarbon fuels, lead to lower NO_x emissions when compared to premixed configurations. A lower concentration of O/H radicals under rich conditions leads to altered reaction pathways, which produce less NO out of NH_i oxidation [23].

Although the HPDF combustion process for ammonia is promising regarding reduced wall quenching effects and different emission characteristics compared to premixed combustion, the unfavorable combustion characteristics of ammonia might inhibit the ignition of the fuel spray. Some aspects of this issue are apparent from the latent heat of vaporization and the heating value of selected fuels in Table 1. The comparison shows that the evaporation of ammonia requires a larger share of its energy content than other fuels. Additional problems result from the above-mentioned low flame speed, high auto-ignition temperature and narrow flammability limits. Therefore, it is unknown whether freely propagating ammonia sprays can be successfully ignited by small diesel pilot injections under engine-relevant conditions.

The work presented in the paper at hand aims to identify the conditions under which HPDF combustion of ammonia is feasible by examining the ignition and combustion characteristics of a single ammonia spray, which is ignited by a diesel pilot. A systematic variation of the temporal and spatial interaction of ammonia and diesel identifies suitable injector configurations and injection strategies. This is achieved by analyzing heat release rates (HRRs) of combustion events in a rapid-compression-expansion-machine (RCEM). Based on a suitable configuration, a variation of charge conditions evaluates the influence of the engine load on HPDF ammonia combustion. In addition, a variation of pilot amount and injection duration identifies the effect of different pilot characteristics and the minimum necessary pilot amount for ammonia ignition at an operating point (OP), which showed fast ammonia ignition and high conversion rates.

2. Experimental setup

The experiments are conducted in a pneumatically driven rapid compression expansion machine, which is described in detail by Dorer et al. [25]. It has already been used to investigate the HPDF combustion of diesel and methane [26,27].

Fig. 1 shows the driving mechanism and the injector arrangement. The RCEM consists of two concentrically arranged ring pistons, which are coupled kinetically by hydraulic oil. When the experiment is started by opening the valves of the driving-air bottles, the outer driving piston is accelerated. Due to coupling via the hydraulic oil, the inner working piston is accelerated into the opposite direction, which cancels the net momentum on the setup and thereby reduces vibrations, which might influence the measured quantities. By compressing the air charge of the cylinder, a dynamic equilibrium is reached and followed by an expansion phase. The design of the hydraulic oil flow orifices influences the trajectory of the working piston and ensures a piston movement similar to an engine. The fuels are injected close to TDC. As only small amounts of fuel are injected, the influence of the combustion event on the piston trajectory is small and therefore neglected. The equivalent engine speed differs slightly between the investigated OPs, due to altered dynamics of the RCEM at different driving pressures (see Table 2). The controls and data acquisition are based on a National Instrument CompactRIO system, which features a field-programmable gate array (FPGA). Therefore, control operations, such as the fuel injection, can be triggered at a certain piston position during the experiment.

The piston movement is not constrained by a crankshaft. This creates the possibility to vary temperature and pressure at TDC independently within a certain range by tuning the driving pressure and the initial charge pressure before compression. Since no charge motion is initiated by the flat piston surface and the roll-up of the boundary layer is suppressed by large piston crevices, as shown in Lee and Hochgreb [28], the gas-core is assumed to stay undisturbed and to undergo adiabatic compression. The core temperature of the charge can be calculated via:

$$T = T_0 \epsilon_{eff}^{\kappa(T)-1} \tag{1}$$

Cold walls and large crevice volumes lead to significant heat losses during compression. Thus, the effective compression ratio of the adiabatic core is calculated from the pressure ratio:

$$\epsilon_{eff} = \frac{v_0}{v} = \left(\frac{p}{p_0}\right)^{1/\kappa(T)} \tag{2}$$

The total air mass and the global equivalence ratio in the RCEM depend on the initial charge pressure, which differs between the OPs. However, this does not have a direct effect on the combustion event, as only the local interaction between two single fuel sprays is investigated. The investigated operating conditions at TDC of unfired experiments are listed in Table 2 and represent a load range from low-load (OP1) to full-load (OP4) engine conditions. Due to small deviations in driving pressure, initial charge temperature, as well as friction effects due to variations in oil temperature, conditions at TDC vary slightly between single experiments (see Table 2). The estimated error in temperature is calculated via superposition of the effects of initial temperature deviation ($296\,K \pm 1.5\,K$) and the effect of varying TDC pressures on TDC temperatures (see Eqs. (1) and (2)). The initial charge temperature is measured via a thermocouple before the experiment. The error in TDC pressure is based on measured pressure deviations during unfired experiments, which were obtained by a piezo-electric pressure transducer Kistler 7061C.

In accordance with previous investigations on methane/diesel HPDF combustion, two single-hole injectors are used. The fuel sprays interact in a plane parallel to the cylinder head. The ammonia injector can be rotated to obtain different relative spray angles α (see Fig. 1). The diesel injection timing is kept constant at 2 ms before TDC, while the ammonia injection timing is shifted relative to TDC. Thus, the setup allows the variation of the temporal and spatial interaction of the two sprays. As HPDF injectors in four-stroke engines usually only consist of one injector body, the distance between the two nozzles is kept small. While the diesel injection pressure is not adapted to part-load cases, the ammonia injection pressure is adapted to the different back-pressures of the OPs to keep the injected amount of ammonia and the injection time constant. The ammonia injection time and the injected LHV of ammonia match the injection time and the injected LHV of methane in previous works on

Table 1
Characteristics of different fuels. Properties from [24] at 1 bar .

Parameters	Ammonia	Diesel	Methanol
LHV [MJ/kg]	18.8	45.6	19.9
Latent heat of vaporization at 1 bar [kJ /kg]	1371	317	1101
Ratio of latent heat of vaporization to LHV [%]	7.3	0.7	5.5

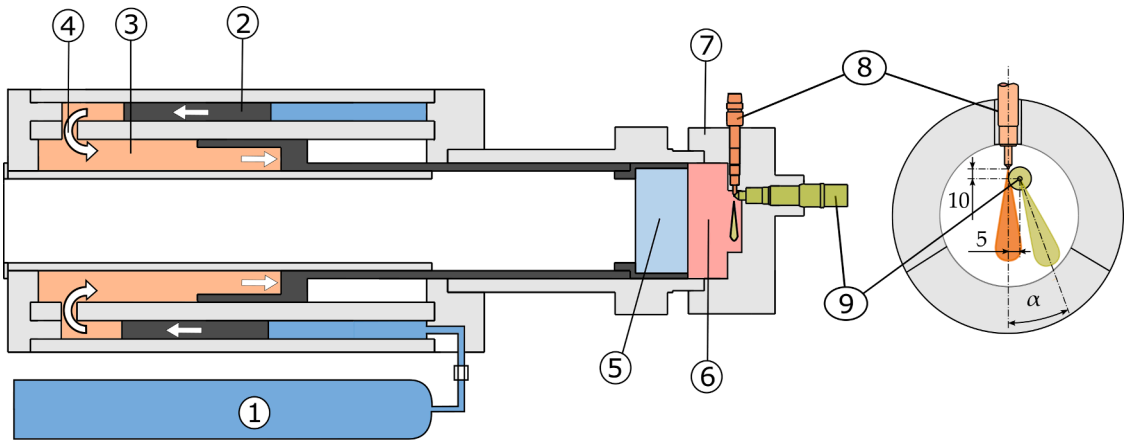

Fig. 1. RCEM driving system and cylinder head: ① driving-air bottles, ② driving piston, ③ hydraulic fluid, ④ flow orifice, ⑤ working piston, ⑥ combustion chamber, ⑦ cylinder head, ⑧ diesel injector, ⑨ ammonia injector.

Table 2
Investigated operating points.

Parameter	OP1	OP2	OP3	OP4
TDC temperature [K]	780 ± 8	829 ± 10	865 ± 10	920 ± 10
TDC pressure [bar]	75 ± 1.5	88 ± 2	98 ± 2	125 ± 2
ϵ_{eff} [−]	12.9	14.6	17.2	20.5
Equivalent engine rpm $[\frac{1}{\text{min}}]$	≈ 800	≈ 880	≈ 920	≈ 1000

methane/diesel HPDF combustion at the test rig. Both injectors were analyzed with an IAV injection analyzer over a wide range of injection pressures and injection durations. The resulting rate profiles were parametrized and approximated by top-hat profiles to allow interpolation between the tested combinations. Two different nozzle tips with orifice diameters of 110 µm and 200 µm, respectively, were attached to a type CRI 2.20 Bosch diesel injector. This permits the variation of the injected diesel amount over a wide range without extremely different injection timings and injection pressures. Important characteristics of the examined diesel injections are shown in Table 3.

Both fuels are supplied by air driven high-pressure pumps. The ammonia injection system is shown in Fig. 2. As cavitation must be avoided during the suction stroke of the ammonia pump, ammonia is pre-pressurized in an intermediate storage tank. This is a similar approach as used by Ryu et al. [20] for ammonia/DME mixtures. A back-pressure valve in the leakage path after the ammonia injector ensures a defined thermodynamic state of ammonia throughout the injector. The ammonia leakage stream is directed into a large water container, which acts as an acid trap. Most components of the fuel supply system are located in a ventilated gas cabinet. A variety of additional safety measures is employed, such as burst-disks, gas-detectors, automatically closing valves as well as a high-performance ventilation system, which reacts on the gas-detectors signal.

An overview of the RCEM specifications and injection parameters is shown in Table 4.

Table 3
Parameters of diesel injections .

Nozzle diameter [µm]	Diesel mass [mg]	Injection pressure [bar]	Injection duration (hydraulic) [µs]	Fraction of LHV [−]
200	10	2000	830	10.0%
200	5	2000	520	5.2%
110	5	2000	1460	5.2%
110	3	2000	850	3.2%
110	1.5	2000	570	1.6%
110	0.9	1100	560	1.0%

3. Heat release rate analysis

The HRR is calculated from the piston position and the pressure signal via a multi-zone thermodynamic model. The model features an isentropic core I, which undergoes isentropic compression and expansion, as proposed by Lee and Hochgreb [28] for a rapid compression machine. Heat losses are calculated based on the model presented in Fink et al. [27]. Heat transfer to the isothermal walls is assumed to occur only in the crevices C, which exchange mass with a gap G, while the isentropic core I does not exchange any mass with the adjacent gap G. The temperature profile along the crevices is modeled by dividing the crevice zone into 8 logarithmically sized crevice elements. The heat loss model is fitted to match the heat loss of the RCEM during unfired experiments at the investigated OPs by adapting the surface area of the crevices. Fig. 3 shows the modeled zones and their interactions.

By explicitly considering the mass fluxes due to fuel injection and the species conversion during combustion, Fink et al. [27] calculated the HRR of the combustion event for methane/diesel HPDF combustion. In the case of ammonia/diesel, diesel pilot fractions are increased due to the unfavorable combustion characteristics of ammonia. Therefore, it becomes more important to differentiate which fuel is being consumed at each time step. This is not possible from the pressure and position signals alone. In addition, the cooling effect of ammonia on the cylinder charge due to the large heat of vaporization cannot be time-resolved coherently. Therefore, the injection of the two fuels, the species conversion during combustion and the evaporation of ammonia are not considered in this model. This approach is common for the calculation of apparent HRRs in direct-injection engines, as the major contribution to the pressure rise is caused by combustion. However, it is to be noted that the neglected effects play a more significant role for ammonia engines than for diesel engines as the heat of vaporization and the injected number of moles are larger. The first law of thermodynamics is used to solve the model for the apparent HRR in the isentropic core, which originates from combustion, fuel injection, evaporation and species conversion. The interaction of hot combustion products with the RCEM walls will lead to heat losses, which are not considered by the fitting to unfired experiments. However, the neglected losses are similar among the conducted experiments and direct comparisons of the HRRs are assumed to be valid. The RCEM setup with cold walls and single fuel sprays is unable to reproduce the late stages of combustion when wall-interaction and the interaction between several fuel sprays influence the combustion process.

Fig. 4 shows an exemplary HRR curve and injection profiles, which were obtained in an experiment at OP4 with converging jets and a slightly advanced diesel injection. Pilot ignition is assumed to occur when the HRR exceeds 0.14 MW compared to the HRR at the time of the

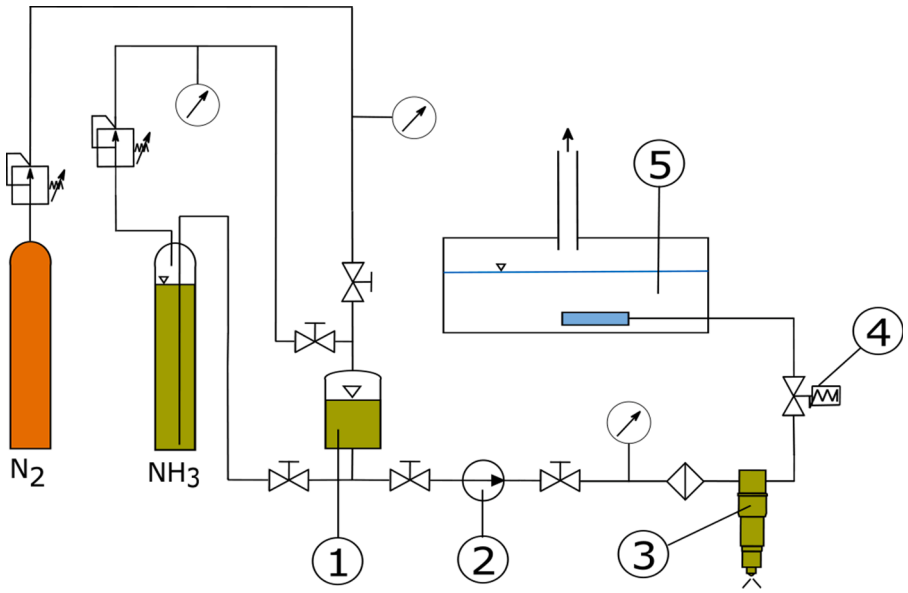

Fig. 2. Ammonia injection system: ① intermediate storage tank, ② ammonia pump, ③ ammonia injector, ④ back-pressure valve, ⑤ acid trap.

Table 4
RCEM specifications and injection parameters .

Bore diameter [mm]	220
Start of diesel injection [ms BTDC]	2
Ammonia injection pressure [bar]	480–530
Ammonia nozzle diameter [µm]	940
Injected ammonia mass [mg]	210
Duration ammonia injection [µs]	2700
Relative ammonia injection timing [µs]	− 1000 – + 1500

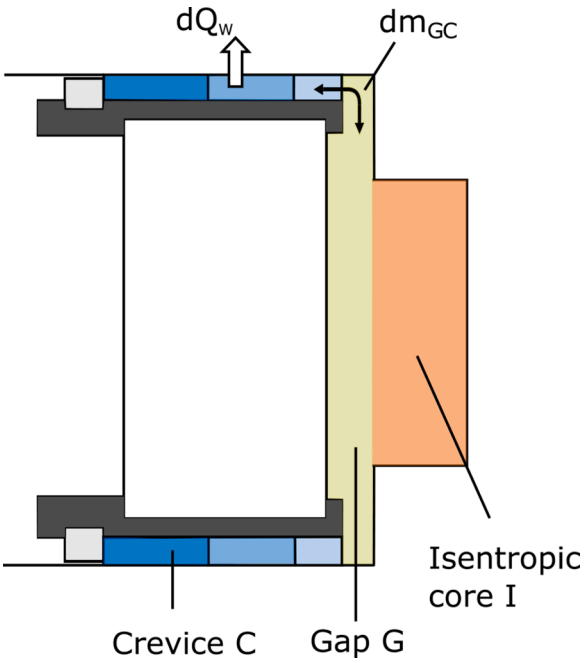

Fig. 3. Thermodynamic model of the combustion chamber.

start of pilot injection. This relative criterion is necessary, as the apparent HRR drops during the evaporation of ammonia for late diesel injections. The diesel ignition delay Δt_p is defined as the time between pilot ignition and pilot start of injection. The main ignition of ammonia is detected via a total threshold value of 0.45 MW and the main ignition delay Δt_m is calculated from the time between the first ammonia injection and the detected main ignition. Misfiring is assumed if the HRR does not exceed the threshold value for main ignition during the combustion process. The relative ignition delay Δt_{mp} is obtained from the time between pilot and main ignition. The relative burnout rate of the injected fuels is calculated by integrating the apparent HRR, normalizing it with the injected LHV of both fuels and subsequently normalizing it with the highest value in the discussed data set. While this does not give an absolute value for the percentage of fuel burnt, it permits a comparison of the presented cases. A comparison with methane and methanol on the same test rig indicates that the highest observed burnout rates of ammonia are similar to the other fuels for OP4.

4. Results

The results section is divided into three parts. At first, the temporal and spatial interaction of diesel and ammonia fuel sprays is varied over a wide range of parameters for two pilot sizes at OP4 to identify suitable geometrical arrangements and injection timings. This is done by comparing fuel burnout rates and ignition delay times. Subsequently, the charge conditions are varied from low to full-load conditions. In the last part, the effects of pilot amount and injection duration are assessed by using two different diesel nozzles.

4.1. Geometrical arrangement and injection timing

Fig. 5 shows the relative burnout rate for relative injection timings ranging from − 1000 µs (ammonia first) to + 1500 µs (diesel first), interaction angles ranging from $\alpha = -22.5°$ (converging) to $\alpha = 15°$ (diverging) and 10 mg (left) or 5 mg (right) diesel pilots. The data set consists of a total of 149 experiments including at least two repetitions for each case, which showed successful ignition. Although the total number of repetitions for each data point is low, significant trends can be clearly identified and the effects of the spray interaction on the combustion of ammonia can be described. Tested combinations are marked with a black dot. Cases in which at least one repetition did not exceed the main ignition threshold are located in the white area. The relative burnout rate is normalized with the data point indicated by a star, which was obtained with a 10 mg pilot, $\alpha = -7.5°$ and a relative injection timing of + 500 µs. This data point showed the highest conversion rate in the set.

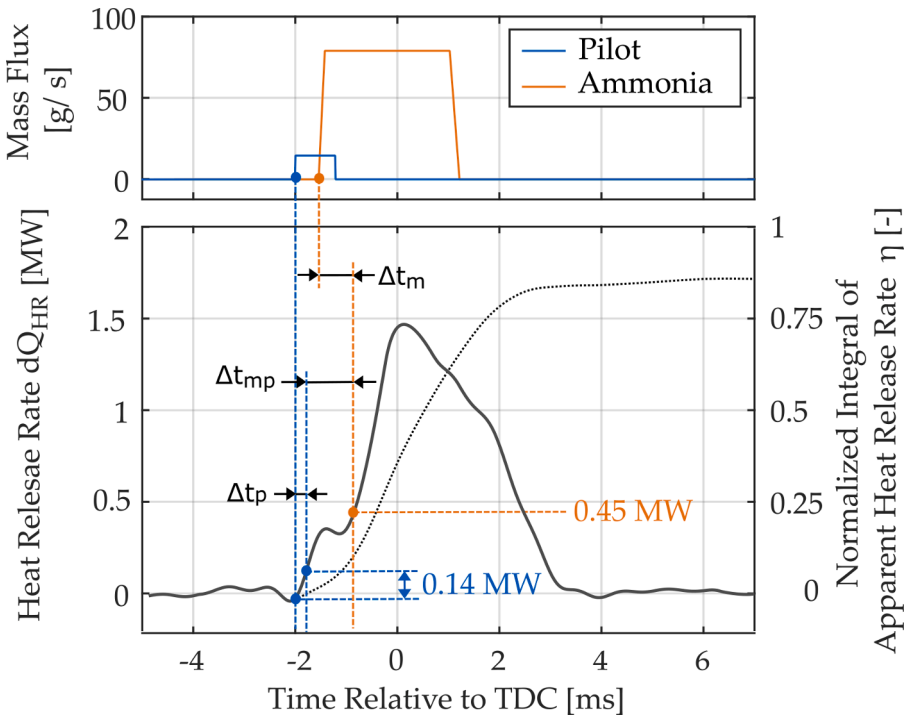

Fig. 4. Determination of key figures from the HRR and injected mass fluxes.

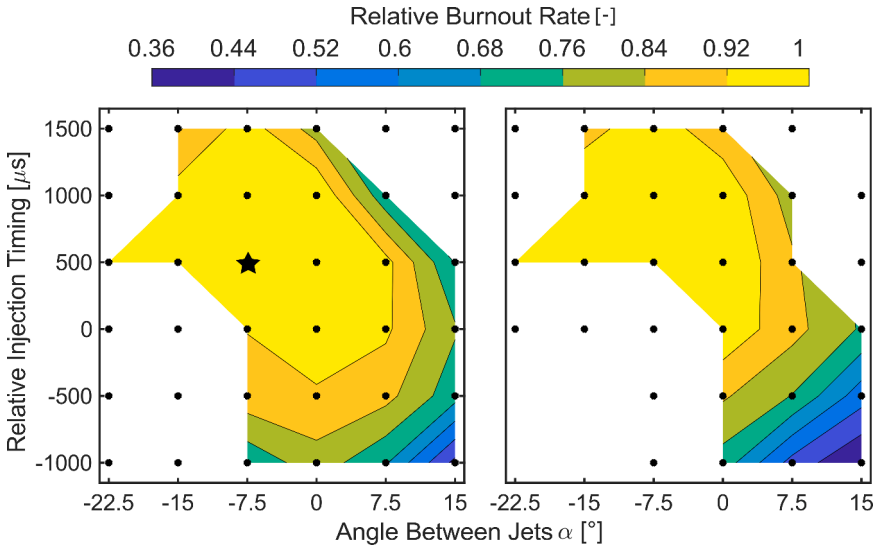

Fig. 5. Relative burnout rate for different interaction angles α and relative injection timings for 10 mg (left) and 5 mg (right) diesel pilots.

Misfiring occurs either in cases with insufficient interaction of the two fuel sprays or in cases where diesel strongly interacts with ammonia. Insufficient interaction is observed for advanced diesel injections combined with diverging or strongly converging ($-$ 22.5°) spray configurations. For negative relative injection timings (ammonia first) and negative, converging interaction angles, the diesel spray is strongly influenced by ammonia and ignition is inhibited. While the 10 mg diesel pilot can ignite the ammonia spray at an interaction angle of $\alpha = -7.5°$ consistently, the region of misfiring is extended for the smaller 5 mg pilot. Although some strongly delayed ignitions were observed in this area for the 5 mg pilot, complete quenching occurred, as well. The quenching can be explained by the strong interaction between diesel and ammonia, which leads to lower air entrainment into the diesel spray. Instead, ammonia is entrained, which has a cooling effect due to its lower temperature, high enthalpy of evaporation and heat capacity. In addition to this physical effect, it has been shown that ignition delay times of n-heptane rise with increasing ammonia fractions [29]. Previous studies on methane/diesel HPDF combustion [26,27] showed no misfiring at full-load charge conditions (OP4). However, at low-load conditions (OP1), similar observations were made. Even at low-load conditions the ignition was still possible for a wider range of interaction angles and relative injection timings than for ammonia, although a smaller diesel pilot was used. The small range of interaction cases in which ammonia ignition occurs suggests that a larger minimum amount of energy has to be delivered to the ammonia spray compared to methane in order to reliably initiate main ignition.

The relative burnout rate is high for parallel or converging sprays and moderately advanced diesel injections. These conditions permit an

undisturbed ignition of the diesel pilot, which is followed by a strong interaction with the ammonia spray. While the relative burnout rate for the 5 mg pilots is lower compared to the 10 mg pilots for negative relative injection timings, it is similarly high for positive relative injection timings. For the investigated conditions, the effect of altering spatial and temporal interaction of the two sprays is far larger than the effect of increasing pilot size.

Pilot, main and relative ignition delays are shown in Fig. 6. Pilot ignition delays are similar for advanced diesel injections and diverging sprays, as an undisturbed pilot ignition is possible. For parallel or converging sprays combined with a negative relative injection timing (ammonia first), diesel ignition is deteriorated by ammonia and a significant increase in pilot ignition delay is observed before pilot ignition is completely inhibited and misfiring occurs. Particularly high pilot ignition delays are observed for simultaneous injection of both fuels. The tip region of gaseous jets and liquid fuel sprays is characterized by a leading vortex in which less air is entrained [30,31]. This might increase the inhibiting effect of ammonia on diesel ignition. A similar behavior of the pilot ignition delay has been observed at low-load conditions (OP1) for methane/diesel HPDF combustion [26].

Short main ignition delays are observed for strong spatial spray interactions due to converging sprays and advanced diesel injections. A strong correlation between main ignition delay and relative burnout rate (Fig. 4) shows that early ammonia ignition is necessary to achieve high burnout rates for the investigated conditions. This could be explained by quenching of the ammonia spray on the cylinder wall, if ignition does not occur early enough. The quenching might be weaker for real engines, as the walls are not as cold as the RCEM walls. The pilot variation decreases the main ignition delay only slightly.

Relative ignition delays are generally shorter for stronger spray interaction. As expected, the relative ignition delay increases approximately with the difference in time between the two injections for positive relative injection timings (diesel first). Interestingly, for negative relative injection timings, the relative ignition delay mainly depends on the interaction angle α and not on the relative injection timing. However, the relative burnout rate (Fig. 4) decreases for a decrease in relative injection timing in this area. While the ignition process of diesel and the subsequent transition to ammonia combustion are only mildly affected by a change of the relative injection timing, a large part of the injected ammonia is not converted. This can be explained by an interaction of the earlier injected ammonia with the cylinder walls and corroborates the hypothesis that quenching on the cylinder wall plays a major role if ignition does not occur shortly after ammonia injection. Similar to the other investigated delay times, the effect of the pilot size is rather small.

4.2. Charge conditions

An operation at part-load conditions of engines using the HPDF combustion process could be realized by only injecting diesel. Nonetheless, in order to substitute as much diesel as possible, injecting ammonia at part-load conditions would further reduce greenhouse gas emissions. The apparent HRRs relative to the start of injection (SOI) of ammonia at OP2–OP4 with identical injection mass fluxes of diesel and ammonia are shown in Fig. 7. The data is obtained by using an interaction angle of $\alpha = -7.5°$ and a slightly advanced 10 mg diesel pilot ($+$ 500 µs), which is the configuration marked by a star in the figures of the previous section. Based on the results in the previous section, it would have also been reasonable to choose further advanced diesel pilots. However, when operating a full-scale engine, strongly advanced diesel injections might not be desirable, e.g., due to thermodynamic considerations. Furthermore, the injected amount of ammonia would not necessarily be kept constant at part-load conditions in a full-scale engine. This is done here to isolate the effect of the charge conditions on the combustion behavior. The HRRs are based on three repetitions each. Instead of discussing key figures, such as ignition delays, the focus is shifted to discussing the HRRs itself. The key figures might be influenced by the different operating conditions, e.g., by a higher degree of premixing of the diesel pilot at less reactive conditions, which causes an HRR that would exceed the main ignition threshold.

While ammonia ignition is successful for OP2–OP4, no ignition was observed at OP1. Although diesel injection starts before ammonia injection, the evaporating ammonia spray is able to inhibit diesel ignition completely. The ammonia spray seems to outrun the diesel pilot during the longer pilot ignition delay and deteriorates pilot ignition at OP1. The first peak of the HRRs of OP2–OP4 is caused by pilot ignition, which is shifted backwards at less reactive charge conditions, due to longer ignition delays. The second, larger peak is mainly caused by the combustion of ammonia. While the pilot peak HRRs slightly increases for less reactive charge conditions due to increased premixing, the main peaks of the HRRs decrease. In addition, the main combustion is shifted significantly more backwards than what was to be expected only from longer pilot ignition delays. This suggests a poor combustion behavior of ammonia at part-load conditions.

Apart from chemical kinetics, different charge conditions influence the ammonia/air mixture formation process significantly. Due to lower charge temperatures, increased mixing is necessary to evaporate and heat up the ammonia spray. In addition, as shown by Naber and Siebers [32], a decrease in charge density leads to increased penetration and less air entrainment. For low-load charge conditions, both effects will lead to a larger influence of wall quenching effects, which is additionally promoted by the cold walls of the RCEM.

4.3. Pilot size

HRRs and corresponding diesel injection mass fluxes resulting from experiments with different piloting strategies (see Table 3) are shown in Fig. 8. The shown HRRs are based on three repetitions each and obtained at OP4 with $\alpha = -7.5°$ and slightly advanced $+$ 500 µs diesel pilots. This interaction case showed fast ammonia ignition and high conversion rates.

The larger 200 µm nozzle leads to a faster rise of the HRR and a broader profile, indicating more diffusive combustion compared to the 110 µm nozzle. In particular, the two 5 mg diesel pilot injections illustrate that the shorter injection with a higher mass flux leads to a steeper rise of the HRR, i.e. a more intense onset of ammonia combustion. While the ignition delay is lower for the larger nozzle, the overall combustion duration is shorter for the smaller nozzle. Depending on the desired combustion characteristics, one of the two shapes might be favored. The HRRs obtained with 10 mg and 5 mg 200 µm injections are similar, apart from the expected faster rise in HRR when employing a larger pilot. Ignition of ammonia is possible for pilots as small as 1.5 mg, which equals a fraction of 1.6 % of the total injected LHV. However, a reduction of the pilot size below 3 mg (LHV fraction of 3.2 %) leads to a slow rise of the HRR and quenching on the cylinder wall seems to become dominant. Therefore, only a significantly smaller fraction of the heat release of the other cases is observed for the 1.5 mg pilot. No clear peak of the HRR can be identified for the 1 mg injection, although some combustion occurs.

Apart from the injected mass, the investigated diesel injection scenarios differ in a variety of properties, such as penetration, spray angle and injection duration. Therefore, an unambiguous explanation for the observed differing combustion behavior is hardly possible. Although the presented findings might be specific to the investigated interaction case and operating point, the study shows that the pilot characteristics influence the combustion behavior of the ammonia spray significantly. In that regard, the HPDF combustion of ammonia is different from methane, as the HRR of methane could be mainly correlated to the degree of premixing before main ignition [27].

5. Conclusions

The suitability of ammonia as a fuel for HPDF combustion was

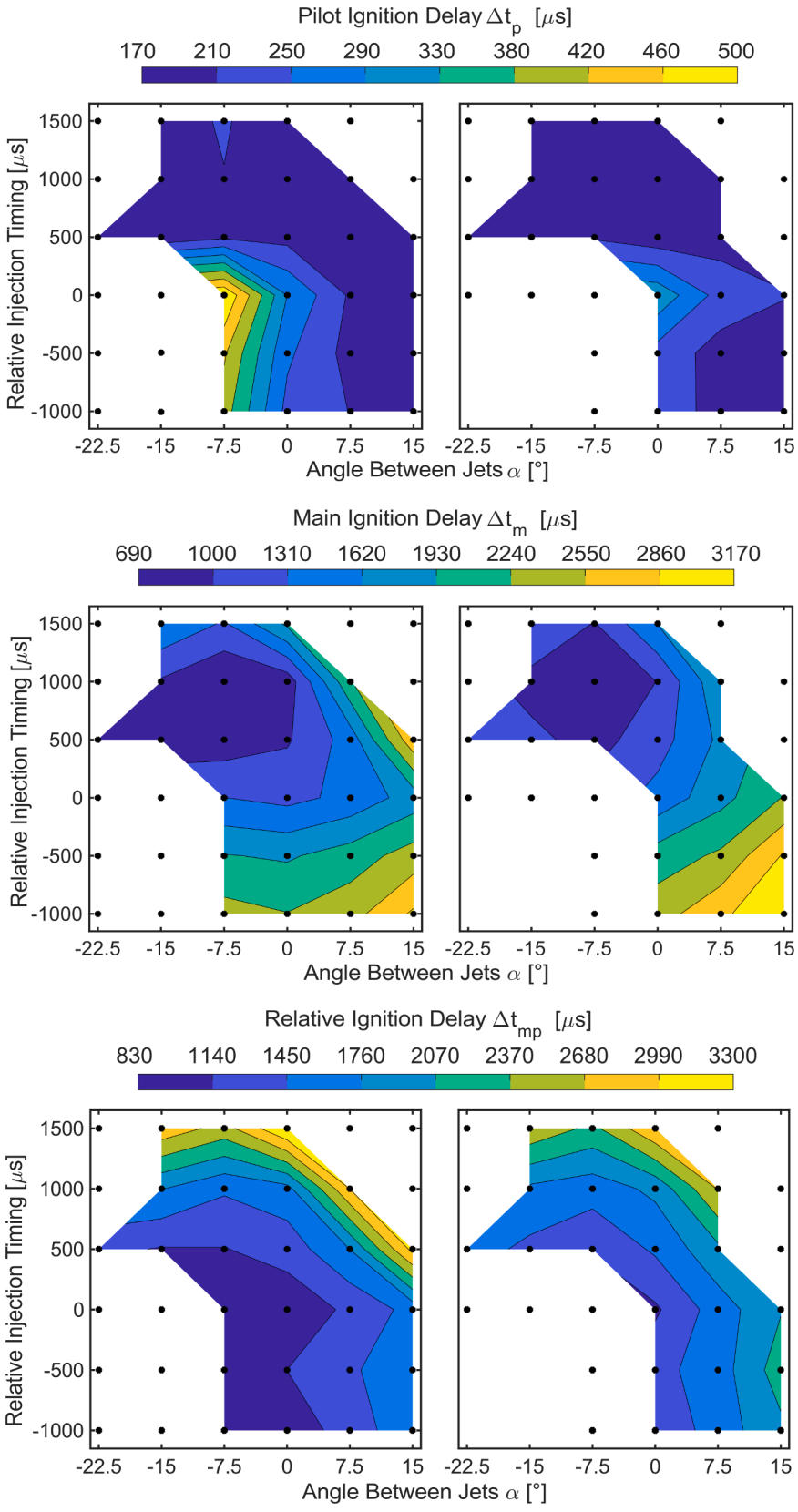

Fig. 6. Pilot, main and relative ignition delay for different interaction angles α and relative injection timings for 10 mg (left) and 5 mg (right) diesel pilots.

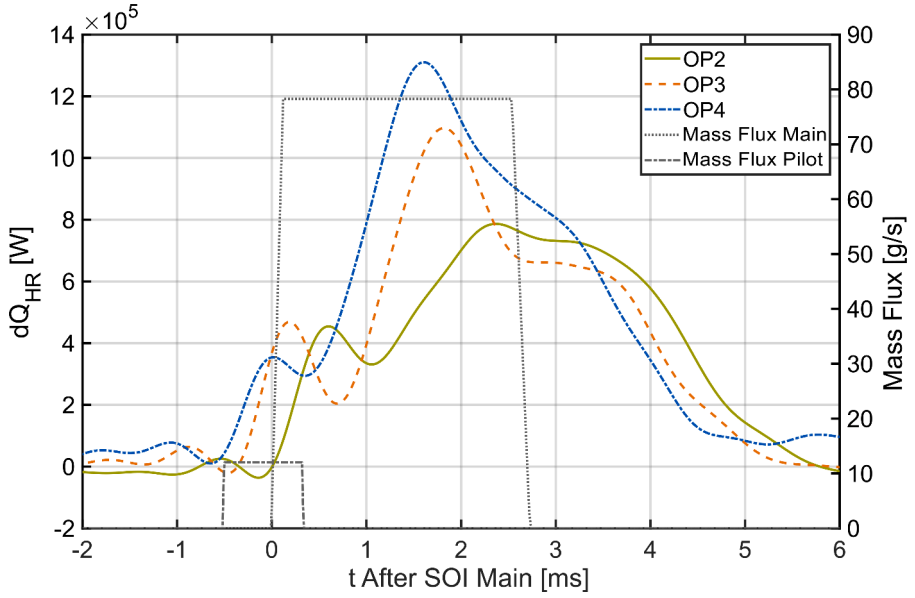

Fig. 7. Fuel mass fluxes and averaged apparent HRRs for different operating points with slightly advanced (+ 500 µs) 10 mg diesel injections and converging sprays ($\alpha = -7.5°$).

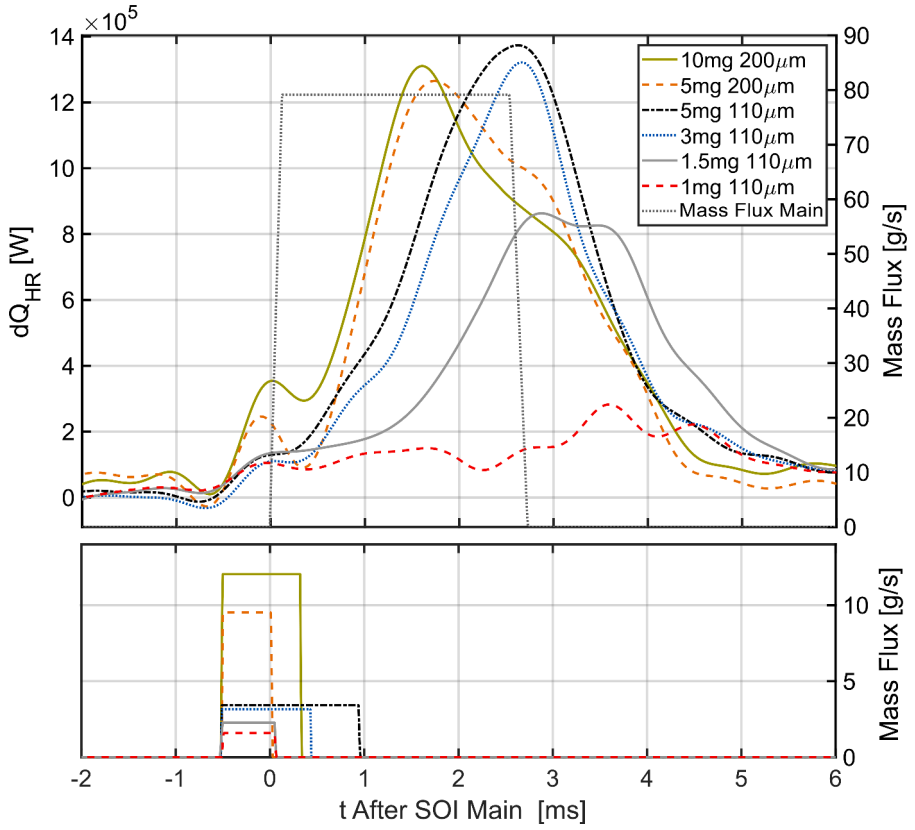

Fig. 8. Diesel mass fluxes (bottom), ammonia mass flux (top) and averaged apparent HRRs (top) for different, slightly advanced (+ 500 µs) diesel pilots at OP4 and converging sprays ($\alpha = -7.5°$).

investigated in an RCEM by examining single ammonia sprays, which interact with small diesel pilots at engine-relevant conditions. A variation of the spatial and temporal interaction of the two sprays was carried out by altering the interaction angle and the relative injection timing. Key figures, such as a normalized conversion rate and ignition delay times, were derived from the apparent HRR, which was obtained by the thermodynamic modeling of the combustion chamber. The following effects were revealed:

- The ammonia spray is able to inhibit the diesel pilot ignition even at full-load engine conditions, if the sprays interact strongly before pilot ignition occurs (i.e. converging sprays and simultaneous/delayed diesel injection). An increase in pilot ignition delay was observed, when approaching cases in which misfiring occurred. This indicates

that the deteriorating effect of ammonia on diesel ignition gradually increases until pilot ignition fails entirely. A similar behavior was observed for methane at low-load conditions, as a comparison with previous investigations at the test-rig shows [27].

- The highest ammonia burnout rates are achieved for strong spatial interaction (i.e., converging sprays) and advanced diesel pilots. With such configurations, the ammonia spray interacts intensely with the already ignited diesel pilot and burns in a mainly diffusive manner.
- A strong correlation between main ignition delay and relative burnout rate hints at a significant influence of wall quenching if the ammonia spray does not ignite early enough. However, due to the cold walls of the RCEM, this effect may be significantly stronger than in a real engine.

Subsequently, a range of charge conditions representing low to full engine load was investigated for a favorable spatial and temporal interaction case by comparing the obtained apparent HRRs. Both pilot and main ignition delay increased for less reactive conditions and misfiring occurred in the least reactive case. The overall lower HRR indicates lower conversion rates and a generally poor suitability of ammonia HPDF combustion for low-load conditions.

Finally, the effect of different pilot injection strategies was studied. The analysis of the HRRs yielded the following key findings:

- Reliable ignition of ammonia is possible using a pilot with an LHV fraction as small as 3.2 % for the investigated conditions.
- The ammonia ignition delay increases for smaller pilot amounts.
- For the investigated cases, short pilot injection durations with high mass flux reduce ignition delay and intensify the onset of ammonia combustion.

In general, the RCEM study indicates that HPDF combustion of ammonia is feasible for application in real engines, and the development of multi-jet engine injectors and subsequent engine testing is encouraged. The combustion process is found to be sensitive to the interaction between the fuel sprays, charge conditions and pilot characteristics. Although less near-wall quenching is generally considered an advantage of HPDF combustion, the RCEM study has shown that heat release of ammonia may suffer from wall quenching effects, if the investigated parameters are not chosen carefully. The full engine injector should guarantee a high degree of interaction between ammonia and diesel sprays. In order to avoid quenching at the cylinder wall, measures to increase air entrainment into the ammonia sprays are recommended. Possible measures are, e.g., increasing the spray angle and injecting the same mass flux through more nozzles [32]. In addition, the compression ratio of a suitable test engine should be high. Due to the employed injector arrangement with only two single hole injectors, which leads to very low energy input, and the properties of the RCEM, like absence of swirl and low wall temperatures, real engines may perform significantly better than to be expected on the basis of the presented results.

Declaration of Competing Interest

The authors declare that they have no known competing financial interests or personal relationships that could have appeared to influence the work reported in this paper.

Acknowledgments

This research is funded by the German Federal Ministry for Economic Affairs and Climate Action on the basis of a decision by the German Bundestag (project no. 03SX534D), which is gratefully acknowledged. The authors would like to acknowledge the support of the AmmoniaMot consortium (Woodward L'Orange, MAN Energy Solutions, WTZ Rolau and Neptun Ship Design). Furthermore, the authors would like to express their sincere gratitude to Georg Fink, Utkarsh Pathak and Tomislav Lackovic for their support.

References

[1] American Bureau of Shipping. Ammonia as marine fuel: sustainability whitepaper. 2020. https://absinfo.eagle.org/acton/media/16130/sustainability-whitepaper-ammonia-as-marine-fuel.
[2] Garabedian C. G., Johnson J. H.. The theory of operation of an ammonia burning internal combustion engine. https://apps.dtic.mil/sti/citations/AD0634681.
[3] Niki Y, Nitta Y, Sekiguchi H, Hirata K. Emission and combustion characteristics of diesel engine fumigated with ammonia. Proceedings of the ASME internal combustion engine fall technical conference - 2018. New York, N.Y.: The American Society of Mechanical Engineers; 2019, ISBN 978-0-7918-5198-2. https://doi.org/10.1115/ICEF2018-9634.
[4] Westlye FR, Ivarsson A, Schramm J. Experimental investigation of nitrogen based emissions from an ammonia fueled SI-engine. Fuel 2013;(111):239–47. https://doi.org/10.1016/j.fuel.2013.03.055.
[5] Cornelius W, Huellmantel LW, Mitchell HR. Ammonia as an engine fuel. SAE Trans 1966;(74):300–26.http://www.jstor.org/stable/44460524
[6] Starkman ES, James GE, Newhall HK. Ammonia as a diesel engine fuel: theory and application. SAE Trans 1968:3193–212.http://www.jstor.org/stable/44562852
[7] Lesmana H, Zhang Z, Li X, Zhu M, Xu W, Zhang D. NH_3 as a transport fuel in internal combustion engines: a technical review. J Energy Resour Technol 2019; 141(7). https://doi.org/10.1115/1.4042915.
[8] Dimitriou P, Javaid R. A review of ammonia as a compression ignition engine fuel. Int J Hydrogen Energy 2020;45(11):7098–118. https://doi.org/10.1016/j.ijhydene.2019.12.209.
[9] Ryu K, Zacharakis-Jutz GE, Kong S-C. Performance enhancement of ammonia-fueled engine by using dissociation catalyst for hydrogen generation. Int J Hydrogen Energy 2014;39(5):2390–8. https://doi.org/10.1016/j.ijhydene.2013.11.098.
[10] Comotti M, Frigo S. Hydrogen generation system for ammonia–hydrogen fuelled internal combustion engines. Int J Hydrogen Energy 2015;40(33):10673–86. https://doi.org/10.1016/j.ijhydene.2015.06.080.
[11] Mørch CS, Bjerre A, Gøttrup MP, Sorenson SC, Schramm J. Ammonia/hydrogen mixtures in an SI-engine: engine performance and analysis of a proposed fuel system. Fuel 2011;90(2):854–64. https://doi.org/10.1016/j.fuel.2010.09.042.
[12] Ryu K, Zacharakis-Jutz GE, Kong S-C. Effects of gaseous ammonia direct injection on performance characteristics of a spark-ignition engine. Appl Energy 2014;116: 206–15. https://doi.org/10.1016/j.apenergy.2013.11.067.
[13] Mounaïm-Rousselle C, Mercier A, Brequigny P, Dumand C, Bouriot J, Houillé S. Performance of ammonia fuel in a spark assisted compression ignition engine. Int J Engine Res 2021. https://doi.org/10.1177/14680874211038726.
[14] Gray JT, Dimitroff E, Meckel NT, Quillian RD. Ammonia fuel - engine compatibility and combustion. SAE technical paper series. SAE International; 1966. https://doi.org/10.4271/660156.
[15] Pearsall TJ, Garabedian CG. Combustion of anhydrous ammonia in diesel engines. SAE Trans 1968;(76):3213–21.http://www.jstor.org/stable/44562853
[16] Bro K, Pedersen PS. Alternative diesel engine fuels: an experimental investigation of methanol, ethanol, methane and ammonia in a D.I. diesel engine with pilot injection. SAE technical paper series. SAE International; 1977. https://doi.org/10.4271/770794.
[17] Reiter AJ, Kong S-C. Demonstration of compression-ignition engine combustion using ammonia in reducing greenhouse gas emissions. Energy Fuels 2008;22(5): 2963–71. https://doi.org/10.1021/ef800140f.
[18] Niki Y, Yoo D-H, Hirata K, Sekiguchi H. Effects of ammonia gas mixed into intake air on combustion and emissions characteristics in diesel engine. Proceedings of the ASME internal combustion engine fall technical conference - 2016. New York, N.Y.: The American Society of Mechanical Engineers; 2016, ISBN 978-0-7918-5050-3. https://doi.org/10.1115/ICEF2016-9364.
[19] Gross CW, Kong S-C. Performance characteristics of a compression-ignition engine using direct-injection ammonia–DME mixtures. Fuel 2012;103:1069–79. https://doi.org/10.1016/j.fuel.2012.08.026.
[20] Ryu KH, Zacharakis-Jutz G, Kong S-C. Effects of fuel compositions on diesel engine performance using ammonia-DME mixtures. SAE technical paper series. SAE International; 2013. https://doi.org/10.4271/2013-01-1133.
[21] Pochet M, Jeanmart H, Contino F. A 22:1 compression ratio ammonia-hydrogen HCCI engine: combustion, load, and emission performances. Front Mech Eng 2020; 6. https://doi.org/10.3389/fmech.2020.00043.
[22] Hodgins KB, Hill PG, Ouellette P, Hung P. Directly injected natural gas fueling of diesel engines. SAE technical paper series. SAE International; 1996. https://doi.org/10.4271/961671.
[23] Haynes BS. Reactions of ammonia and nitric oxide in the burnt gases of fuel-rich hydrocarbon-air flames. Combust Flame 1977;28:81–91. https://doi.org/10.1016/0010-2180(77)90010-4.
[24] Linstrom P.. NIST chemistry webbook, NIST standard reference database 69.. 10.18434/T4D303.
[25] Dorer F, Prechtl P, Mayinger F. Investigation of mixture formation and combustion prozesses in a hydrogen fueled diesel engine. In: Saetre TO, editor. Hydrogen power: theoretical and engineering solutions. Dordrecht: Springer Netherlands; 1998, ISBN 978-90-481-5029-8. p. 49–54. https://doi.org/10.1007/978-94-015-9054-9_6.
[26] Fink G, Jud M, Sattelmayer T. Influence of the spatial and temporal interaction between diesel pilot and directly injected natural gas jet on ignition and

combustion characteristics. J Eng Gas Turbine Power 2018;140(10). https://doi.org/10.1115/1.4039934.
[27] Fink G, Jud M, Sattelmayer T. Fundamental study of diesel-piloted natural gas direct injection under different operating conditions. J Eng Gas Turbine Power 2019;141(9). https://doi.org/10.1115/1.4043643.
[28] Lee D, Hochgreb S. Rapid compression machines: heat transfer and suppression of corner vortex. Combust Flame 1998;114(3–4):531–45. https://doi.org/10.1016/S0010-2180(97)00327-1.
[29] Yu L, Zhou W, Feng Y, Wang W, Zhu J, Qian Y, et al. The effect of ammonia addition on the low-temperature autoignition of n-heptane: an experimental and modeling study. Combust Flame 2020;217:4–11. https://doi.org/10.1016/j.combustflame.2020.03.019.
[30] Rizk W. Experimental studies of the mixing processes and flow configurations in two-cycle engine scavenging. Proc Inst Mech Eng 1958;172(1):417–37. https://doi.org/10.1243/PIME_PROC_1958_172_037_02.
[31] Reitz RD, BRacco FV. Ultra-high-speed filming of atomizing jets. Phys Fluids 1979;22(6):1054. https://doi.org/10.1063/1.862711.
[32] Naber J, Siebers DL. Effects of gas density and vaporization on penetration and dispersion of diesel sprays. SAE technical paper series. SAE International; 1996. https://doi.org/10.4271/960034.